Regulation of the Adenomatous Polyposis Coli Gene by the miR-135 Family in Colorectal Cancer

Remco Nagel,[1] Carlos le Sage,[1] Begoña Diosdado,[2] Maike van der Waal,[1] Joachim A.F. Oude Vrielink,[1] Anne Bolijn,[2] Gerrit A. Meijer,[2] and Reuven Agami[1]

[1]The Netherlands Cancer Institute, Division of Tumor Biology and [2]VU University Medical Center, Department of Pathology, Amsterdam, the Netherlands

Abstract

Inactivation of the *adenomatous polyposis coli* (*APC*) gene is a major initiating event in colorectal tumorigenesis. Most of the mutations in *APC* generate premature stop codons leading to truncated proteins that have lost β-catenin binding sites. APC-free β-catenin stimulates the Wnt signaling pathway, leading to active transcription of target genes. In the current study, we describe a novel mechanism for *APC* regulation. We show that miR-135a&b target the 3′ untranslated region of *APC*, suppress its expression, and induce downstream Wnt pathway activity. Interestingly, we find a considerable up-regulation of miR-135a&b in colorectal adenomas and carcinomas, which significantly correlated with low *APC* mRNA levels. This genetic interaction is also preserved in full-blown cancer cell lines expressing miR-135a&b, regardless of the mutational status of *APC*. Thus, our results uncover a miRNA-mediated mechanism for the control of *APC* expression and Wnt pathway activity, and suggest its contribution to colorectal cancer pathogenesis. [Cancer Res 2008;68(14):5795–802]

Introduction

Inactivating mutations in the tumor suppressor gene *Adenomatous Polyposis Coli* (*APC*), a key component of the Wnt signaling pathway, cause formation of adenomas in the large intestine, which are precursors of colorectal cancer (CRC; ref. 1). The malignant transformation process is induced due to subsequent accumulation of genetic alterations, which often include *KRAS* and *p53* mutations, chromosomal gains (e.g., 20q, 13q, and 8q) and losses (17p and 18q), and epigenetic changes (2–4). In the intestine, the canonical Wnt pathway maintains the proliferative compartment at the crypts as well as cell fate and position of the epithelial cells as they differentiate (5). Upon activation of the Wnt pathway, β-catenin is released from the cytoplasmic complex formed by APC, axin, and glycogen synthase 3. Consequently, β-catenin is able to bind the TCF/LEF transcription factors, resulting in transcription of downstream targets such as c-Myc or cyclin D1. In contrast, in differentiated intestinal epithelial cells, APC is acting as a negative regulator of the Wnt signaling pathway by binding to β-catenin to induce its degradation (6). Mice carrying conditional deletions of *APC* or inactivating *APC* mutations develop multiple adenomas in the small intestine (7). In humans, germline mutations in the *APC* gene are found in the majority of Familial Adenomatous Polyposis syndrome, and 60% to 80% of the sporadic colorectal adenomas and adenocarcinomas harbor somatic *APC* mutations (8). Most of the described mutations in *APC* lead to premature stop codons, thereby producing truncated proteins that have lost their β-catenin binding sites (9). Recently, hypermethylation of the promoter region of the *APC* gene has also been described as a mechanism of silencing its expression in sporadic CRC cases (2, 10, 11). In summary, mutations in *APC*, which occur as an early event in CRC development, are a clear initiating event in colorectal adenoma formation.

With the discovery of microRNAs (miRNA), a whole new level of gene regulation was uncovered. These ~20-nucleotide-long noncoding RNAs are able to regulate gene expression posttranscriptionally. They mediate their effects by targeting the RNA-induced silencing complex (RISC) to complementary sites in the 3′ untranslated region (UTR) of their target genes (12). Binding of a miRNA-loaded RISC to a complementary sequence will, depending on the degree of base pairing, either lead to translational repression or decay of the targeted mRNA. In mammalian cells, the complementarity to target sites is generally limited, which hampers the identification of regulated genes.

miRNAs have been shown to play an essential role in diverse processes including development, differentiation, proliferation, and apoptosis (13–18). As such, they have been ascribed oncogenic or tumor suppressive functions (19–22). Several miRNA expression signatures have been reported in CRC (23–26). Yet, specific target genes and pathways, through which these miRNAs might contribute to colorectal carcinogenesis, have not been documented thus far.

Previously, we developed a miRNA expression library (miR-Lib) to identify new miRNA functions (22). This tool enabled us to screen for regulatory miRNAs acting on one specific gene of interest (27). This way, we uncovered the regulation of p27[Kip1] expression by miR-221&222 in glioblastoma (27). Using a similar approach, we in this study attempted to identify miRNAs regulating the *APC* gene (28). We identified miR-135a and miR-135b (miR-135a&b) as regulators of *APC*, and show their potent effect on Wnt pathway activity. Moreover, we show that miR-135a&b are highly expressed in colorectal adenomas and carcinomas, with concomitant low levels of *APC*, suggesting that up-regulation of these miRNAs might be involved in CRC pathogenesis.

Materials and Methods

Cell culture. HeLa, MCF-7, HEK293T, CaCo2, Colo205, DLD-1, HCT15, HT29, LS174T, SW48, SW480, WiDr, and L-cells were cultured in DMEM supplemented with 10% FCS and antibiotics. For miR-135 inhibitor treatment, cells were grown to 30% confluency, after which the tissue culture medium was replaced with medium containing either 25 μmol/L

(24 wells) or 75 μmol/L (6 wells) of miR-135 or control (miR-372) inhibitors. Sequences (Dharmacon) were as follows: 135, Chl-UAG AAU CAC AUA GGA AUG AAA AGC CAU AGA GAA; and 372, Chl-CGG UGA CGC UCA AAU GUC GCA GCA CUU UCC ACU.

L-cells and L-cells stably expressing Wnt3A were a kind gift from A. Berns (NKI, Amsterdam, The Netherlands). Wnt-conditioned medium was harvested as previously described (29).

For the miRNA-library screen, transfection and virus harvesting steps were carried out on a Hamilton ML as described before (27).

Patient material. Frozen and paraffin-embedded tissues of 43 colorectal tumors (23 adenomas and 20 carcinomas) and 18 colorectal normal epithelium from fresh specimens were collected at the Free University medical center (VUmc), Amsterdam. The study was carried out in accordance with the ethical guidelines of our institution concerning informed consent about the use of patient's material after surgical procedures. DNA from the colorectal tumors was isolated from archival paraffin-embedded tissue as previously described (3, 30). Total RNA was isolated using TRIzol (Invitrogen) according to manufacturers protocol with some modifications, described in detail on the VUmc Web site.[3] All tumor samples were reviewed by an expert gastrointestinal pathologist (GAM) and classified according to standard criteria. In addition, tissue areas for DNA and RNA isolation were histologically verified to contain a minimum of 70% tumor.

Constructs. GFP-*APC*-3′UTR was constructed by cloning the 3′UTR of *APC* between EcoRI and BamHI restriction sites of the green fluorescent protein (GFP) sensor vector as described in (27). The 3′UTR of *APC* was amplified from genomic DNA using GCC TCG AGT TAA AAG AGA GGA AGA ATG AAA CTA AG forward and GCG GAT CCG CAT GTA TCT CCA TTG TTT ATG G reverse primers. Genomic DNA was isolated using the QIAamp DNA mini kit (Qiagen) according to the manufacturers instructions.

Luc-*APC*-3′UTR was produced by subcloning the 3′UTR of *APC* into the pGL3 vector (Promega) downstream of the luciferase gene by means of PCR. Primers used for this PCR were GCG ACG TCT TAA AAG AGA GGA AGA ATG AAA CTA AG and CAC CGG TGC ATG TAT CTC CAT TGT TTA TGG as forward and reverse primers, respectively. Luc-*APC*-3′UTR-DM was created using GTA TAC TAT CAA AT*G GAT CC*T CCA GAA CAA AAA CCC and GTA CAA ACA TAC T*GG ATC C*TA CTA TTT TTT TCC TAA CCA TC as primers. Italicized is the miR-135 antiseed sequence converted to BamHI.

The APC[kd] was designed to target the sequence AAT GTC CCT CCG TTC TTA TGG and was constructed as previously described (31).

TOPFLASH and FOPFLASH constructs were a kind gift of A. Berns.

pGL3-M4 was a kind gift of R. Bernards (NKI, Amsterdam, The Netherlands; ref. 32), the corresponding pGL3-M4-mutant was constructed using GCG CTA GCC CAG CTT GCA TGC CTG CAG GTC GAC CCA C*AC ATG T*GT GCC TCC CAC *ACA TGT* GTG CCT CCC ACC *ACA TGT* GTG CCT CCC AC*A CAT GT*G TGC CTC TCG ACT CTA GAG GAT CC as a forward and GCA AGC TTA CTT AGA TCG CAG ATC TCG AGC as a reverse primer. The four E-boxes were mutated to ACATGT, and are italicized in the sequence.

Quantitative reverse transcription-PCR and real-time Taq Man PCR. Total RNA was extracted from cell lines using TRIzol reagent according to manufacturers protocol. Synthesis of cDNA with Superscript III reverse transcriptase (Invitrogen) was primed with oligo(dT). Primers used for detection of *APC* levels (Fwd GGA AGC AGA GAA AGT ACT GGA and Rev CTG AAG TTG AGC GTA ATA CCA G) and *β-actin* (Fwd CCT GGC ACC CAG CAC AAT and Rev GGG CCG GAC TCG TCA TAC T) were designed to amplify 100 to 200 bp fragments. Analyses were carried out using SYBR Green PCR master mix (Applied Biosystems) and the ABI Prism 7000 system (Amersham-Pharmacia). Results were normalized with respect to *β-actin* expression. mRNA levels were quantified according to the δ δ cycle threshold (Ct) method.

Quantification of the *APC* expression levels in tumor samples was measured by reverse transcription-PCR (RT-PCR) using SYBR Green. cDNA was synthesized with Superscript II reverse transcriptase (Invitrogen) using oligo(dT) primers. RT-PCR was performed using primers directed to

APC (Fwd, TGT CCC TCC GTT CTT ATG GAA; Rev, TCT TGG AAA TGA ACC CAT AGG AA) and the house keeping gene β*2M* (Fwd, TGA CTT TGT CAC AGC CCA AGA TA; Rev, AAT GCG GCA TCT TCA AAC CT). Reactions were conducted *in duplo* in a 7300 Real-time PCR System (Applied Biosystems).

Taq Man miRNA assays (Applied Biosystems) that include RT primers and Taq Man probes were used to quantify the expression of mature miRNA-135a (AB: 4373140) and miRNA-135b (AB: 4373139) in cell lines and tumor tissue samples. Gene expression was calculated relative to 18S rRNA (AB: 4333760F), glyceraldehyde-3-phosphate dehydrogenase (AB: 4333764), or the RNU48 gene (AB: 4373383). Expression levels were calculated from the Ct values obtained from triplicate PCRs (33). Differences in expression levels between controls and the tumor samples were evaluated by the Kruskal-Wallis and Mann-Whitney *U* nonparametric test for independent samples (SPSS 14.0 for Windows; SPSS, Inc.).

Western blot analysis and antibodies. Proteins were analyzed by SDS-PAGE and Western blotting using Immobilon-P transfer membrane (Millipore). For loading control, an antibody against tubulin was used (YL1/2; European Collection of Animal Cell Cultures). Antibodies against β-catenin, active β-catenin (dephosphorylated), and APC were a kind gift of M. Fornerod (NKI, Amsterdam, The Netherlands).

Luciferase assay. Luciferase assays were performed as described before (34). In short, MCF-7 cells were transfected using PEI (Polysciences, Inc). For Luc-*APC*-3′UTR reporter assays, cells were cultured in 24-well plates and transfected with 5 ng Luc-*APC*-3′UTR (or DM), 5 ng Renilla, and 0.5 μg of miR-135a, miR-135b or APC[kd].

For TOP/FOP assays, HEK293T cells were cultured in 24-well plates and transfected either with 100 ng TOP- or FOPFLASH, 5 ng Renilla, and 0.5 μg of miR-135a, miR-135b, or APC[kd].

Myc activity was measured using pGL3-M4 and pGL3-M4-mut. HEK293T cells were transfected with 100 ng of the Myc-reporter constructs, 5 ng Renilla, and 0.5 μg of miR-135a, miR-135b, or APC[kd]. In all instances, luciferase activity was measured 72 h after transfection using the Dual-luciferase reporter assay system (Promega).

Flow cytometry. The separation of low-GFP-expressing miR-Lib-containing cells was performed by cell sorting using the FACSAria cell sorter from Becton Dickinson. The validation of miRNA hits was performed as described before (27), using HeLa cells stably expressing GFP-*APC*-3′UTR.

APC mutation analysis. *APC* mutation status was analyzed by sequencing the mutation cluster region (MCR) between codons 1286 and 1513 in all colorectal tumor and control samples. To cover the MCR region, four primers sets (set 1: Fwd CAG ACT TAT TGT GTA GAA GA, Rev CGC TCC TGA AGA AAA TTC AAC; set 2: Fwd GA GCT GGC AAT CGA ACG ACT, Rev GAA GTT CCA GCA GTG TCA CAG C; set 3, Fwd GCT CAG ACA CCC AAA AGT CC, Rev ATT TTT AGG TAC TTC TCG CTT G; and set 4, Fwd AA ACA CCT CCA CCA CCT CC, Rev C ATT CCC ATT GTC ATT TTC C) were used for PCR reactions as previously described (2). The PCR products were inspected by running on a 2% agarose gel, after which the products were purified using SAP and EXO enzymes. Subsequently, samples were prepared for sequencing using the ABI PRISM BigDye terminator cycle sequencing ready kit (Applied Biosystems) according to manufacturers protocol. Sequencing was done on a 3130 DNA sequencer (Applied Biosystems) and analyses were carried out with the sequencer navigator and the Vector NTI (Invitrogen).

APC promoter methylation analysis. Promoter methylation of the *APC* gene was established by methylation-specific PCR (MSP). Before MSP, samples were subjected to sodium bisulfite treatment according to the EZ DNA Methylation kit (Zymo Research Coorporation) using 500 ng of DNA as starting material. Primer sequences to amplify the methylated alleles comprised Fwd TAT TGC GGA GTG CGG GTC and Rev TCG ACG AAC TCC CGA CGA and, for the unmethylated alleles, Fwd GTG TTT TAT TGT GGA GTG TGG GTT and Rev CCA ATC AAC AAA CTC CCA ACA A. All MSP reactions included bisulfite-treated DNA from the Colo205 cell line as positive control for unmethylated alleles and DNA derived from human placenta, and treated *in vitro* with *Sss*I methyltransferase (New England Biolabs) for the methylated alleles. All MSP products were inspected by running on a 2% agarose gel containing ethidium bromide.

---

[3] http://www.vumc.nl/microarrays/index.html

Results

APC expression is suppressed by miR-135a and miR-135b. To identify miRNAs that directly regulate the expression of *APC*, we made use of a previously developed sensor vector (27) and cloned the 3′UTR of *APC* downstream of the *GFP* gene. HeLa cells were transduced with this vector, and a single clone stably expressing GFP-*APC*-3′UTR was isolated and expanded. Subsequently, we transduced the cell line with the miRNA vectors (miR-Vec) from our miR-Lib, drug selected, and pooled all stable clones. We assumed that miRNAs that regulate APC expression through its 3′UTR will reduce the fluorescent signal, enabling us to distinguish between *APC*-targeting and nontargeting miRNAs (Fig. 1*A*). After 2 weeks in culture, the low-GFP-expressing cells were fluorescence-activated cell sorting (FACS)-sorted from the total GFP-expressing cell population, and genomic DNA was extracted from both populations. By comparing the relative abundance of miR-Vec inserts between low and total GFP-expressing populations using our miR-Arrays, we were able to identify 5 miR-Vecs that were reproducibly enriched in the low-GFP-expressing population (Fig. 1*B*).

We next tested the effect of each of these miRNAs by comparing their regulatory capacity on either GFP-*APC*-3′UTR or a GFP-control-3′UTR. Whereas miR-135a&b inhibited GFP-*APC*-3′UTR expression by ∼35%, no effect was observed toward a control GFP-3′UTR construct (Fig. 1*C*). For the other obtained hits

(miR-19b, 199a, and 371), no significant down-regulation of the GFP-*APC* reporter could be detected (Supplementary Fig. S1). Subsequently, we subcloned the 3′UTR of *APC* downstream of a luciferase gene, creating luc-*APC*-3′UTR. Transient expression of this vector revealed that miR-135a&b reduce luciferase expression levels by ∼30% to 40% when compared with control miR-Vec (Fig. 1*D*).

To determine whether miR-135a&b affect endogenous *APC* expression, we transduced HEK293T cells, which possess a wild-type Wnt signaling pathway, with the miR-Vec constructs. The expression of miR-135a and miR-135b were verified using quantitative reverse transcription-PCR (qRT-PCR; Supplementary Fig. S2).

Examination of endogenous APC protein levels from HEK293T cells stably expressing miR-135b revealed a clear down-regulation of APC protein compared with cells expressing a control construct (Fig. 2*A*). A corresponding reduction in *APC* mRNA levels was detected by qRT-PCR, suggesting mRNA decay as a mechanism involved in miR-135a&b–mediated APC regulation (Fig. 2*B*).

Examination of the *APC* 3′UTR for miR-135a&b binding sites revealed two potential target sequences. TargetScan 4.0 predicted the first site, whereas the second site was obtained using RNA22 software (Fig. 2*C*). To show specificity of miR-135 function, we mutated both sites, generating a double mutant (DM) of the luciferase reporter (Fig. 2*D*). Cotransfection experiments revealed that the DM is completely refractory to miR-135a&b–mediated
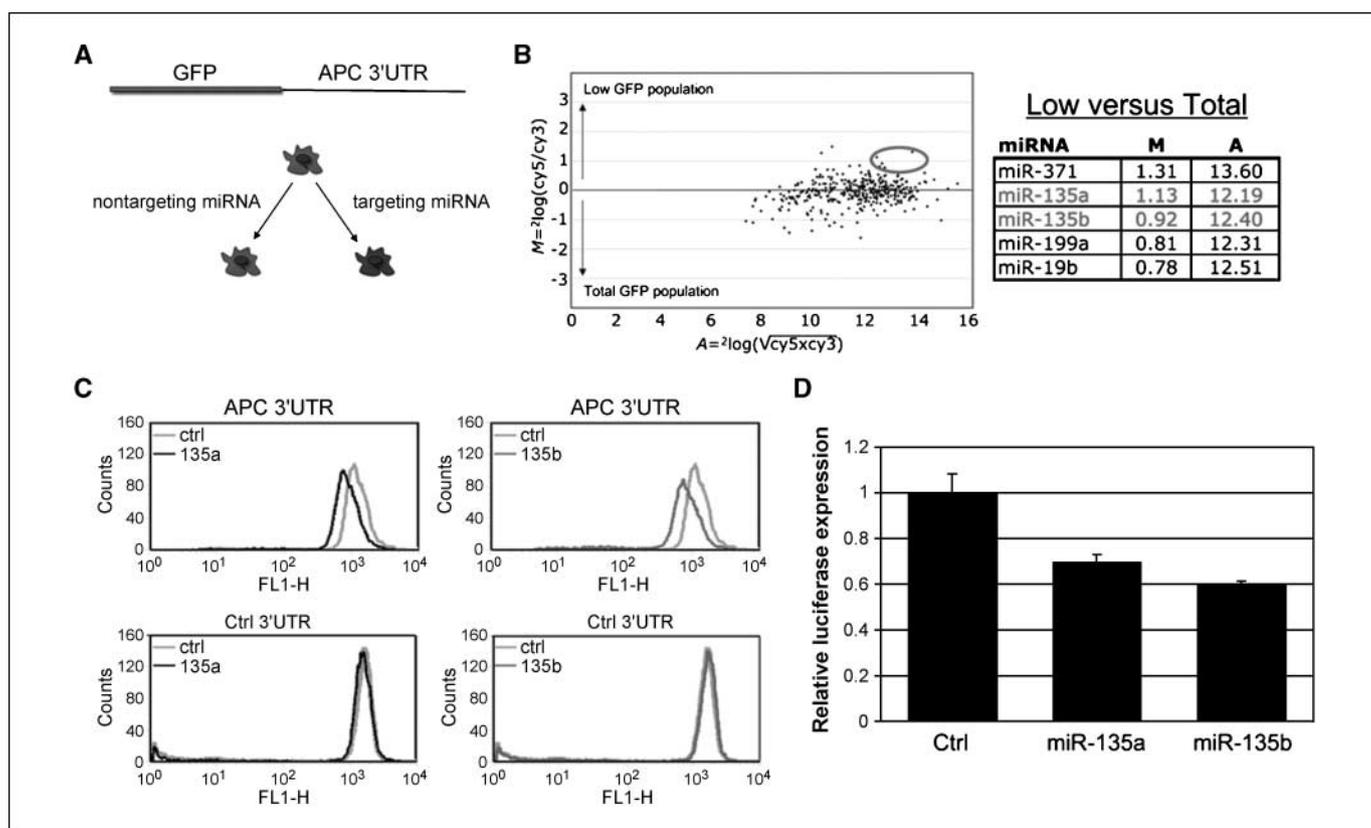

Figure 1. Identification of miR135a&b regulatory capacities toward *APC* by a direct target approach. *A,* a schematic representation of the setup of the direct target approach, possible regulators of the *APC* 3′UTR are isolated by FACS sorting of the low GFP population. *B,* a representative MA-plot, showing the relative abundance of each individual miR-Vec in the low and total GFP populations. *Circle,* top outliers. *Right,* a table showing the five common miRNA outliers, which were more abundant in the low GFP population in a duplicate screen are shown. *C,* verification of the effect of miR-135a&b on GFP expression in HeLa GFP-*APC*-3′UTR and control cells by FACS. GFP expression of control (*ctrl*)-expressing (miR-Vec-hTR) and miR-expressing cells are indicated in different colors. *D,* dual luciferase assay showing relative expression of Luc-*APC*-3′UTR upon transfection with control or miR-135a&b miR-Vecs. Values were normalized to control-transfected cells. A representative figure is shown of at least three independent experiments; *columns,* mean of a triplicate transfection; *bars,* SE.
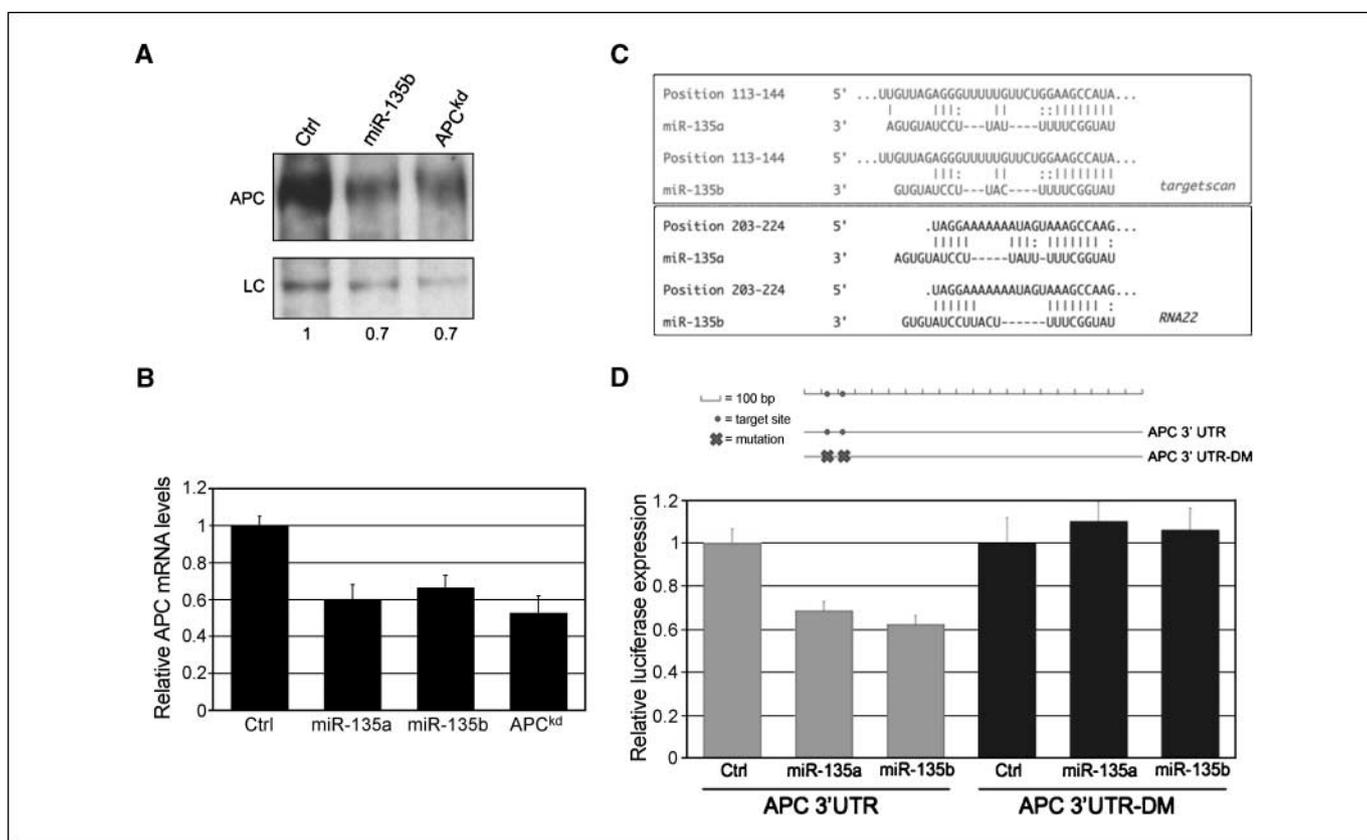
Figure 2. Regulation of endogenous *APC* and the identification of target sites for the miR-135 family. *A,* Western blot showing endogenous APC levels in HEK293T cells stably expressing miR-Vec control, miR-Vec-135b, or pRetroSuper-APC (*APC^kd*). *LC,* loading control staining with tubulin antibodies. *B,* relative mRNA levels in HEK293T cells expressing the indicated constructs as determined by qPCR. Values were normalized to β-*actin* levels. The figure shown is a representative experiment of three independent qPCRs; *columns,* mean of triplicate PCRs, standardized to the control; *bars,* SE. *C,* representation of the target sites identified for miR135a&b by Targetscan 4.0 and RNA22 prediction programs. *D,* schematic representation of the *APC*-3′UTR-DM, and a luciferase experiment showing the effect of miR-135a&b on *APC*-3′UTR and *APC*-3′UTR-DM in MCF-7 cells. A representative figure is shown of at least three independent experiments; *columns,* mean of a triplicate transfection; *bars,* SE.

repression, indicating the direct suppression of *APC* by miR-135a&b (Fig. 2*D*). Altogether, we have identified miR-135a&b as potent regulators of *APC* expression.

miR-135a and miR-135b induce β-catenin signaling. Next, we investigated the functional relevance of the interaction between miR-135a&b and *APC* by determining the effects of their expression on the activity of the Wnt pathway. First, we examined effects of miR-135 on TCF transcriptional activity. Therefore, we transfected HEK293T cells with luciferase reporter constructs harboring either three optimal TCF binding sites (TOPFLASH) or three mutated TCF binding sites (FOPFLASH). Addition of Wnt ligand to cells containing TOPFLASH, but not FOPFLASH, resulted in a 2-fold increase in luciferase counts, demonstrating the activity and specificity of these reporter constructs (Fig. 3*A*). Interestingly, transfection of either miR-135a or miR-135b significantly increased TOPFLASH reporter activity by 1.5-fold, in the absence of Wnt ligand. In comparison, transfection of a functional shRNA construct targeting *APC* (APC^kd) similarly increased TOPFLASH activity by 1.5-fold (Fig. 3*A*). Second, we examined effects of miR-135 on the activated, unphosphorylated form of β-catenin (ABC). In concordance with the above findings, we found that introduction of miR-135a&b increased ABC levels by 1.5-fold compared with control (Fig. 3*B*). This effect was comparable with the APC^kd and in a manner similar to the addition of Wnt ligand. Last, we examined the induction of c-Myc activity, an important downstream target

gene in the Wnt pathway (35). We used luciferase reporter constructs containing promoters under the control of either four Myc responsive elements (M4) or four mutated Myc responsive elements (M4-mut). We observed a 1.5-fold increase in M4 reporter activity, but not M4-mut, in cells cotransfected with miR-135a&b or APC^kd (Fig. 3*C*). Thus, the expression of miR-135a&b activates the Wnt pathway in a manner similar to APC loss and comparable with addition of Wnt ligand.

miR-135a&b suppress APC in CRC cell lines. In all the experiments performed thus far, miR-135a&b were exogenously introduced. To examine whether endogenous miR-135a&b regulate *APC* in a full-blown cancer environment, we first determined the expression level of miR-135a&b in a set of nine CRC cell lines, as *APC* is frequently deregulated in CRC. These cell lines harbor different types of *APC* mutations (listed in Supplementary Table S1). Figure 4*A* shows that all of the CRC cell lines we examined express high levels of miR-135a and miR-135b relative to the control cell lines HeLa and HEK293T.

Next, to inactivate miR-135a&b, we designed one antagomiR that is able to target both miR-135 family members. We tested the effectiveness and specificity of antagomiR-135 on the down-regulation of luciferase-*APC*-3′UTR by miR-135a&b. Supplementary Fig. S3 shows that treatment of antagomiR-135, but not control antagomiR-372, inhibited both miR-135a and miR-135b function, indicating that antagomiR-135 is effective and specific.

Having validated antagomiR-135 as a potent and specific inhibitor of both miR-135a&b, we applied it to the CRC cell lines for 72 hours. Figure 4B shows that in all cases, *APC* mRNA levels were increased 1.5- to 2.5-fold after treatment with antagomiR-135. The observed effect is specific, as *APC* mRNA levels were not altered after antagomiR-135 treatment in cells that do not express miR-135a&b (HeLa and HEK293T). This shows that *APC* is still under control of the miR-135 family members in colorectal cell lines expressing miR-135a&b, regardless of the mutational status of the gene.

miR-135 family expression is increased during CRC progression. To further investigate the role of miR-135a and miR-135b in CRC tumorigenesis, the expression of miR-135a and miR-135b was determined in 43 colorectal tumors (20 adenocarcinomas and 23 adenomas) and 18 controls (normal colon epithelium). The tumors showed an increased expression of both miR-135a and miR-135b compared with normal colon epithelium. We observed a 4.8-fold higher expression of miR-135a ($P < 0.0001$; Fig. 5A) and 10-fold higher expression of miR-135b ($P < 0.0001$; Fig. 5B), in accordance with the previously detected high levels of miR-135a&b expression in the cell lines. Furthermore, we detected a 3.2-fold increase in miR-135a expression levels in colorectal adenomas compared with the controls ($P < 0.0001$), whereas adenocarcinomas showed 6.7 times increased expression ($P < 0.0001$) compared with the control group. Moreover, we found a 2.1 times higher expression of miR-135a in colorectal carcinomas compared with adenomas ($P = 0.007$; Fig. 5C). For miR-135b, we observed a 6.6-fold higher expression in adenomas ($P < 0.0001$) and a 14 times increased expression in the carcinomas ($P < 0.0001$) compared with the control group. The expression of miR-135b was 2.1-fold higher in carcinomas than in adenomas ($P = 0.02$; Fig. 5D). These results imply a role of both miR-135a and miR-135b in the pathogenesis of CRC.

To confirm the connection of the miR-135 family with *APC* gene expression that was observed in the *in vitro* experiments, we measured *APC* mRNA expression levels in this same panel of colorectal samples. As expected, *APC* expression levels were 20 times higher in the normal controls than in the adenomas ($P < 0.008$) and in carcinomas ($P = 0.01$), which is inverse to the pattern that we observed for miR-135a and miR-135b (Fig. 5C and D).

To explore a possible association between the presence of mutations and/or hypermethylation of the *APC* gene and the levels of the miRNAs, we compared the expression levels of both miRNAs in tumors without any aberrations in the *APC* gene to tumors showing mutations and/or hypermethylation events in the *APC* gene. No significant associations between the presence of *APC* mutations and/or promoter hypermethylation, and the expression levels of miR-135a&b in the tumor samples were found (data not shown).

In conclusion, increasing expression of miR-135a and miR-135b from normal colorectal epithelium, through adenomas to adeno-carcinomas, is correlated with decreasing expression of *APC* gene during colorectal tumorigenesis. This association is independent of the status of *APC* mutation or promoter hypermethylation in the tumors.

Discussion

Using a functional genetic screening approach, we have uncovered a novel mechanism for the control of Wnt pathway activity. We identified the miR-135 gene family as a regulator of *APC* expression and showed its potential to activate the Wnt

pathway in the absence of Wnt ligand. Using CRC cell lines, we showed direct and causal suppression of endogenous *APC* by miR-135a&b. Furthermore, in a significant number of colon tumors, we observed high levels of miR-135a&b that negatively correlated with *APC* expression.

miRNAs in control of Wnt signaling. Our study reveals the effect of miR-135 on Wnt signaling in human cells. Recently, Silver and colleagues (36) also identified a miRNA capable of regulating the Wnt pathway in *Drosophila*. Using an unbiased approach to identify miRNAs involved in the Wingless-Wnt pathway, miR-315 was shown to regulate both Axin and Notum, thereby activating the signaling cascade. However, the regulation of the *Drosophila APC* by miR-135a&b was not identified, as these miRNAs are not conserved. Additionally, the regulation of *APC* by miR-135a&b seems a regulatory mechanism specific to humans, as the target
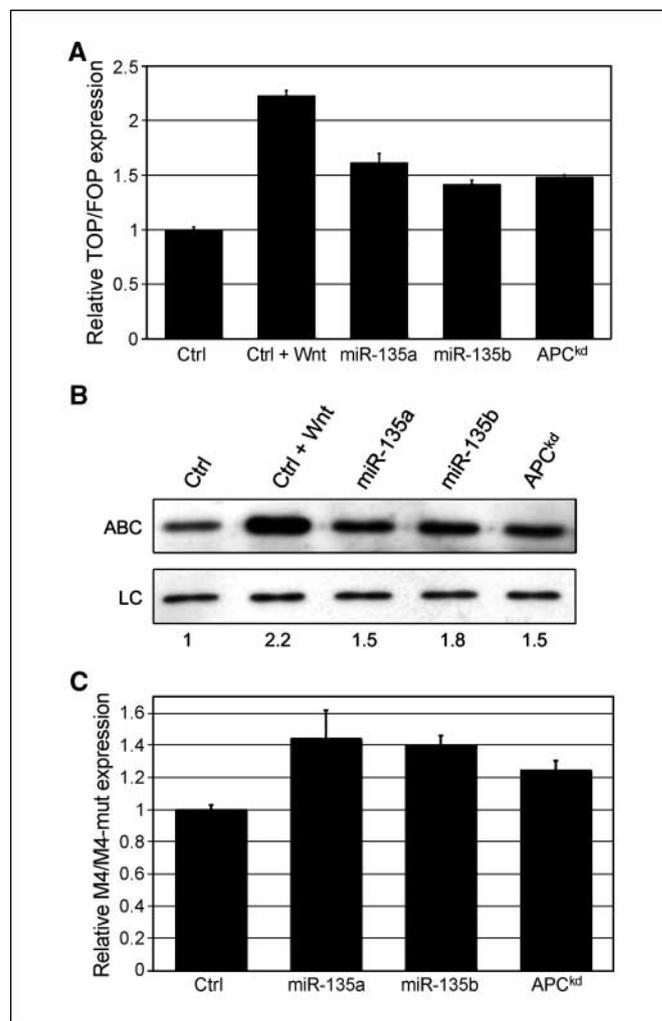

Figure 3. Effects of miR-135a&b expression on Wnt pathway activity. *A,* dual luciferase experiment demonstrating the effect on TOPFLASH/FOPFLASH reporter activity in HEK293T cells. Values were normalized to a Renilla transfection control and standardized to the control vector. The figure shown is a representative of at least three independent experiments. *Columns,* mean of a triplicate transfection; *bars,* SE. *B,* Western blot showing staining of ABC in HEK293T cells stably expressing the indicated constructs. ABC levels were normalized to a tubulin loading control using Tina 2.0 software, and standardized to the control. *C,* dual luciferase assay showing the effect of miR-135a&b expression on a c-Myc reporter construct in HEK293T cells. A representative figure is shown of at least three independent experiments; *columns,* mean of a triplicate transfection; *bars,* SE.

sites for miR135a&b are not conserved in other species (data not shown). Altogether, the observations of Wnt pathway regulation by miR-315, as well as miR-135a&b family, add additional layers to the control of Wnt pathway activity.

Deregulated expression of miR-135 gene family in CRC. To fully understand the role of miR-135a&b in colorectal pathogenesis, it will be necessary to identify the mechanisms regulating expression of these miRNAs. Interestingly, miR-135b is located in the first intron of the *LEM domain containing 1* (*LEMD1*) gene. Although the function of this gene is not known, it has been reported to be highly expressed in CRC compared with control tissue (37). It seems likely that miR-135b will follow the same expression pattern as its host gene and is elevated by the same mechanism. As miR-135b is located on 1q32.1, which frequently shows DNA copy number gain in CRC progression (38, 39), a gene dosage effect could explain the increase in its expression. miR-135a, on the other hand, is encoded by two copies in the human genome, which are located in the first intron of the *stabilin 1* (*STAB1*) gene on 3p21 and in intron 5 of the *rhabdomyosarcoma 2–associated transcript* (*RMST*) gene on 12q23, respectively. To our knowledge, these genes have not been reported to be differentially expressed in CRC or associated with DNA copy number changes during CRC progression. Therefore, the

mechanism by which the miR-135 family is up-regulated in CRC pathogenesis remains to be explored. Nevertheless, our findings suggest that elevation of miR-135 levels is a commonly occurring event in CRC pathogenesis.

Pathway addiction and the miR-135 family. Our results indicate that even in fully developed cancer cells, the presence of miR-135a&b suppresses *APC* expression even when *APC* mutations are present. According to the Knudson hypothesis and the caretaker/gatekeeper model, two hits would suffice to knock down APC function and up-regulate Wnt signaling as a first step toward CRC. The present data, however, suggest that miR-135a&b up-regulation modifies Wnt signaling independent of accumulation of *APC* mutation or promoter methylation status. The observation that high miRNA-135 expression is also found in samples bearing biallelic *APC* mutations might suggest that other targets of this miRNA could also be important for CRC pathogenesis. Additionally, miR-135 expression might work in synergy with *APC* mutations, to inhibit APC function to a greater extent. Similar observations supporting this hypothesis have been made for other regulators of Wnt signaling, such as SFRP1. SFRP1 is frequently inactivated, which is also independent of *APC* mutation or promoter hypermethylation status and results in increased Wnt signaling (40). The term pathway addiction has been suggested for this phenomenon
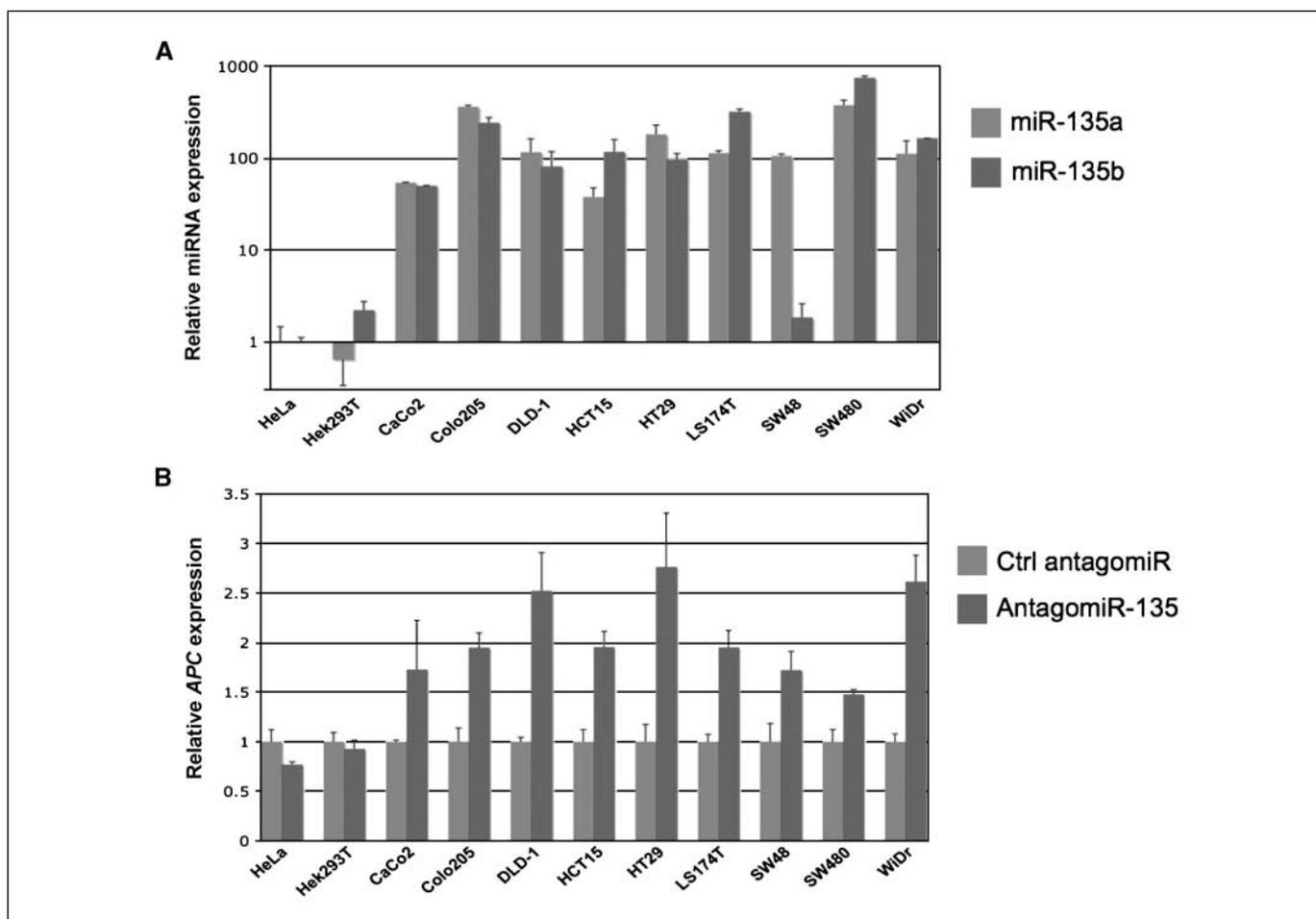

Figure 4. The effect of inhibition of the miR-135 family on *APC* mRNA levels and cellular growth. *A,* relative expression of miR-135a&b in the indicated cell lines as determined by qPCR. Levels were obtained from triplicate PCRs and normalized to the expression levels observed in HeLa cells. Expression of miR-135a and miR-135b is indicated in different colors. miRNA expression is depicted on a logarithmic scale. *B,* relative *APC* mRNA expression 72 h after addition of control or miR-135 antagomiRs as determined by qPCR. Figure is a representative of three independent qPCRs. *Columns,* mean of a triplicate PCR, standardized to the *APC* levels of control antagomiR-treated cells; *bars,* SE.
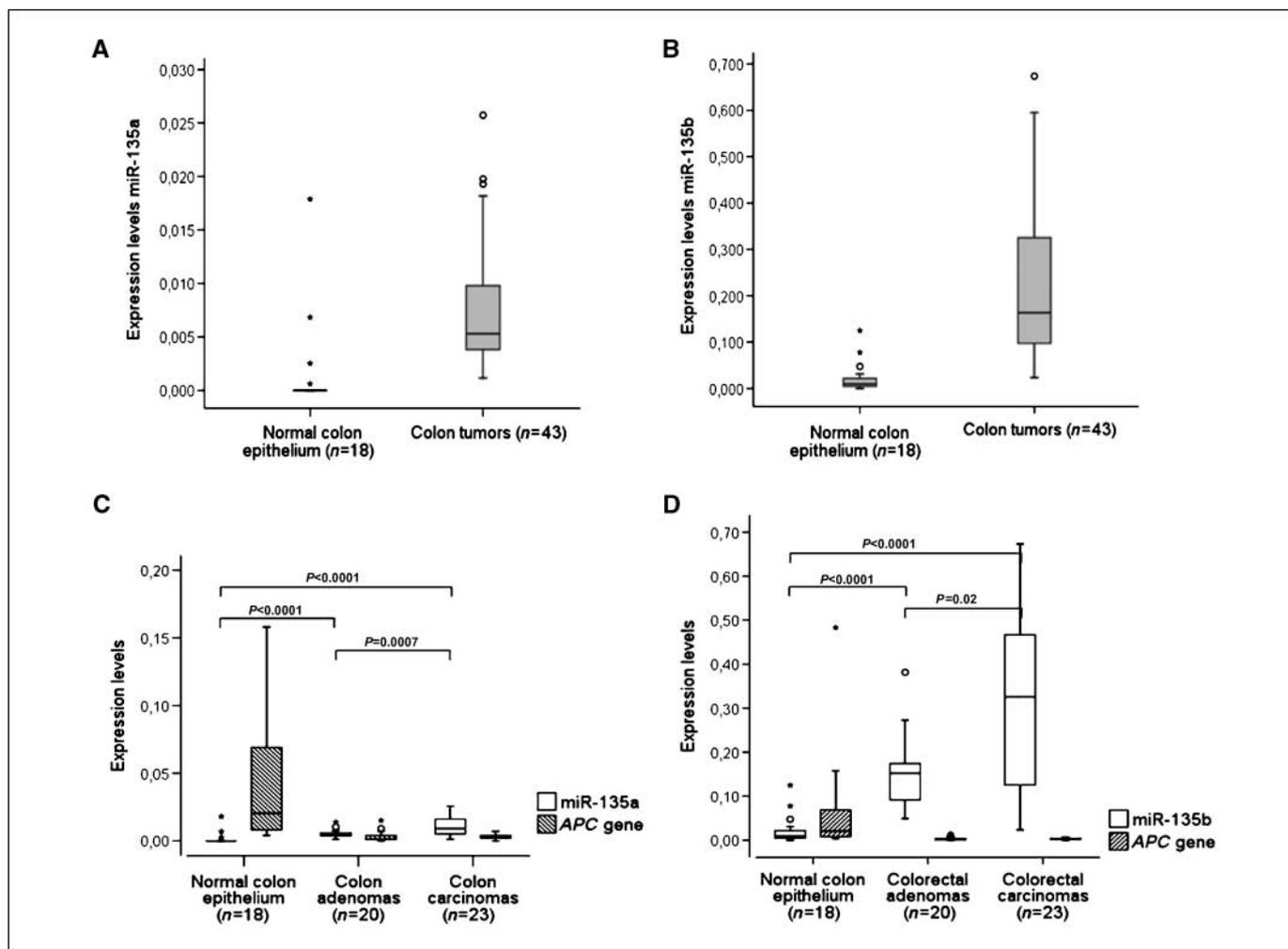
Figure 5. RNA expression levels of miR-135a, miR-135b, and *APC* in 43 colorectal tumors (20 adenocarcinomas and 23 adenomas) and 18 normal colon epithelium samples. *A,* box plots with median, 25th and 75th percentiles, and range of expression levels of miR-135a in 18 normal colon epithelium and 43 colorectal carcinomas showed 4.8-fold significant increased expression of miR-135a in the colorectal tumors ($P < 0.0001$), independently of their histologic status. *B,* box plots with median, 25th and 75th percentiles, and range of expression levels of miR-135b in 18 normal colon epithelium and 43 colorectal carcinomas showed 10-fold higher significant expression of miR-135b in the colorectal tumors ($P < 0.0001$), independently of their histologic status. *C,* box plots with median, 25th and 75th percentiles, and range of expression levels of miR-135a and *APC* mRNA in 18 normal colon epithelium 23 adenomas and 20 carcinomas showed 2.1-fold increased expression of miR-135a in the carcinomas compared with the adenomas ($P = 0.007$) and 6.7-fold increased compared with the controls ($P < 0.0001$). miR-135a expression was twice increased in the adenomas compared with controls ($P < 0.0001$). *D,* box plots with median, 25th and 75th percentiles, and range of expression levels of miR-135b and *APC* mRNA in 18 normal colon epithelium 23 adenomas and 20 carcinomas showed 14-fold increased expression of miR-135b in the carcinomas ($P < 0.0001$) and 6.6 higher expression in the adenomas ($P < 0.0001$) compared with the controls and 2.1-fold increased in the carcinomas compared with the adenomas ($P = 0.02$).

where multiple (epi)genetic alterations cooperate to shift signaling pathways toward a pro-oncogenic direction (41, 42). Our data might imply that elevated miR-135a&b expression is another player in the pathway addiction mechanism, and possibly cooperates with the currently known mechanisms for *APC* deregulation, or is a prerequisite for their efficient occurrence.

Disclosure of Potential Conflicts of Interest

No potential conflicts of interest were disclosed.

Acknowledgments

References

1. Powell SM, Zilz N, Beazer-Barclay Y, et al. APC mutations occur early during colorectal tumorigenesis. Nature 1992;359:235–7.

2. Derks S, Postma C, Moerkerk PT, et al. Promoter methylation precedes chromosomal alterations in colorectal cancer development. Cell Oncol 2006;28:247–57.

3. Hermsen M, Postma C, Baak J, et al. Colorectal adenoma to carcinoma progression follows multiple pathways of chromosomal instability. Gastroenterology 2002;123:1109–19.

4. Fearon ER, Vogelstein B. A genetic model for colorectal tumorigenesis. Cell 1990;61:759–67.

5. Sancho E, Batlle E, Clevers H. Live and let die in

the intestinal epithelium. Curr Opin Cell Biol 2003;15: 763–70.

6. Clevers H. Wnt/β-catenin signaling in development and disease. Cell 2006;127:469–80.

7. Sansom OJ, Reed KR, Hayes AJ, et al. Loss of Apc *in vivo* immediately perturbs Wnt signaling, differentiation, and migration. Genes Dev 2004;18:1385–90.

8. Kinzler KW, Vogelstein B. Lessons from hereditary colorectal cancer. Cell 1996;87:159–70.

9. Rubinfeld B, Albert I, Porfiri E, Munemitsu S, Polakis P. Loss of β-catenin regulation by the APC tumor suppressor protein correlates with loss of structure due to common somatic mutations of the gene. Cancer Res 1997;57:4624–30.

10. Esteller M, Sparks A, Toyota M, et al. Analysis of adenomatous polyposis coli promoter hypermethylation in human cancer. Cancer Res 2000;60:4366–71.

11. Arnold CN, Goel A, Niedzwiecki D, et al. APC promoter hypermethylation contributes to the loss of APC expression in colorectal cancers with allelic loss on 5q. Cancer Biol Ther 2004;3:960–4.

12. Bartel DP. MicroRNAs: genomics, biogenesis, mechanism, and function. Cell 2004;116:281–97.

13. Zhao Y, Ransom JF, Li A, et al. Dysregulation of cardiogenesis, cardiac conduction, and cell cycle in mice lacking miRNA-1–2. Cell 2007;129:303–17.

14. Chen CZ, Li L, Lodish HF, Bartel DP. MicroRNAs modulate hematopoietic lineage differentiation. Science 2004;303:83–6.

15. Lee RC, Feinbaum RL, Ambros V. The C. elegans heterochronic gene lin-4 encodes small RNAs with antisense complementarity to lin-14. Cell 1993;75: 843–54.

16. Wightman B, Ha I, Ruvkun G. Posttranscriptional regulation of the heterochronic gene lin-14 by lin-4 mediates temporal pattern formation in C. elegans. Cell 1993;75:855–62.

17. Reinhart BJ, Slack FJ, Basson M, et al. The 21-nucleotide let-7 RNA regulates developmental timing in Caenorhabditis elegans. Nature 2000;403:901–6.

18. Brennecke J, Hipfner DR, Stark A, Russell RB, Cohen SM. bantam encodes a developmentally regulated microRNA that controls cell proliferation and regulates the proapoptotic gene hid in Drosophila. Cell 2003;113: 25–36.

19. Johnson SM, Grosshans H, Shingara J, et al. RAS is regulated by the let-7 microRNA family. Cell 2005;120: 635–47.

20. He L, Thomson JM, Hemann MT, et al. A microRNA polycistron as a potential human oncogene. Nature 2005;435:828–33.

21. O'Donnell KA, Wentzel EA, Zeller KI, Dang CV, Mendell JT. c-Myc-regulated microRNAs modulate E2F1 expression. Nature 2005;435:839–43.

22. Voorhoeve PM, le Sage C, Schrier M, et al. A genetic screen implicates miRNA-372 and miRNA-373 as oncogenes in testicular germ cell tumors. Cell 2006; 124:1169–81.

23. Volinia S, Calin GA, Liu CG, et al. A microRNA expression signature of human solid tumors defines cancer gene targets. Proc Natl Acad Sci U S A 2006;103: 2257–61.

24. Lanza G, Ferracin M, Gafa R, et al. mRNA/microRNA gene expression profile in microsatellite unstable colorectal cancer. Mol Cancer 2007;6:54.

25. Bandres E, Cubedo E, Agirre X, et al. Identification by Real-time PCR of 13 mature microRNAs differentially expressed in colorectal cancer and non-tumoral tissues. Mol Cancer 2006;5:29.

26. Cummins JM, He Y, Leary RJ, et al. The colorectal microRNAome. Proc Natl Acad Sci U S A 2006;103: 3687–92.

27. le Sage C, Nagel R, Egan DA, et al. Regulation of the p27(Kip1) tumor suppressor by miR-221 and miR-222 promotes cancer cell proliferation. EMBO J 2007;26: 3699–708.

28. le Sage C, Nagel R, Agami R. Diverse ways to control p27(Kip1) function: miRNAs come into play. Cell Cycle 2007;6:2742–9. Epub 2007 Aug 16.

29. Shibamoto S, Higano K, Takada R, Ito F, Takeichi M, Takada S. Cytoskeletal reorganization by soluble Wnt-3a protein signalling. Genes Cells 1998;3:659–70.

30. Weiss MM, Hermsen MA, Meijer GA, et al. Comparative genomic hybridisation. Mol Pathol 1999;52:243–51.

31. Brummelkamp TR, Bernards R, Agami R. A system for stable expression of short interfering RNAs in mammalian cells. Science 2002;296:550–3.

32. Berns K, Hijmans EM, Bernards R. Repression of c-Myc responsive genes in cycling cells causes G1 arrest through reduction of cyclin E/CDK2 kinase activity. Oncogene 1997;15:1347–56.

33. Livak KJ, Schmittgen TD. Analysis of relative gene expression data using real-time quantitative PCR and the 2(-ΔΔ C(T)) Method. Methods 2001;25: 402–8.

34. Kolfschoten IG, van Leeuwen B, Berns K, et al. A genetic screen identifies PITX1 as a suppressor of RAS activity and tumorigenicity. Cell 2005;121:849–58.

35. He TC, Sparks AB, Rago C, et al. Identification of c-MYC as a target of the APC pathway. Science 1998;281: 1509–12.

36. Silver SJ, Hagen JW, Okamura K, Perrimon N, Lai EC. Functional screening identifies miR-315 as a potent activator of Wingless signaling. Proc Natl Acad Sci U S A 2007;104:18151–6.

37. Yuki D, Lin YM, Fujii Y, Nakamura Y, Furukawa Y. Isolation of LEM domain-containing 1, a novel testis-specific gene expressed in colorectal cancers. Oncol Rep 2004;12:275–80.

38. Jones AM, Douglas EJ, Halford SE, et al. Array-CGH analysis of microsatellite-stable, near-diploid bowel cancers and comparison with other types of colorectal carcinoma. Oncogene 2005;24:118–29.

39. Douglas EJ, Fiegler H, Rowan A, et al. Array comparative genomic hybridization analysis of colorectal cancer cell lines and primary carcinomas. Cancer Res 2004;64:4817–25.

40. Caldwell GM, Jones C, Gensberg K, et al. The Wnt antagonist sFRP1 in colorectal tumorigenesis. Cancer Res 2004;64:883–8.

41. Baylin SB, Ohm JE. Epigenetic gene silencing in cancer - a mechanism for early oncogenic pathway addiction? Nat Rev Cancer 2006;6:107–16.

42. Kinzler KW, Vogelstein B. Cancer–susceptibility genes. Gatekeepers and caretakers. Nature 1997;386: 761, 3.

Regulation of the Adenomatous Polyposis Coli Gene by the miR-135 Family in Colorectal Cancer

Remco Nagel, Carlos le Sage, Begoña Diosdado, et al.

Updated version	Access the most recent version of this article at: http://cancerres.aacrjournals.org/content/68/14/5795
Supplementary Material	Access the most recent supplemental material at: http://cancerres.aacrjournals.org/content/suppl/2008/11/12/68.14.5795.DC1

Cited articles	This article cites 42 articles, 12 of which you can access for free at: http://cancerres.aacrjournals.org/content/68/14/5795.full#ref-list-1
Citing articles	This article has been cited by 27 HighWire-hosted articles. Access the articles at: http://cancerres.aacrjournals.org/content/68/14/5795.full#related-urls

E-mail alerts	Sign up to receive free email-alerts related to this article or journal.
Reprints and Subscriptions	To order reprints of this article or to subscribe to the journal, contact the AACR Publications Department at pubs@aacr.org.
Permissions	To request permission to re-use all or part of this article, use this link http://cancerres.aacrjournals.org/content/68/14/5795. Click on "Request Permissions" which will take you to the Copyright Clearance Center's (CCC) Rightslink site.